Actas de las XXXVI Jornadas de Automática, 2 - 4 de septiembre de 2015. Bilbao
ISBN 978-84-15914-12-9

CONTACT SENSORS FOR GIFU HAND III BASED ON FORCE SENSING RESISTORS

Joaquín Blanco Sánchez
Universidad Carlos III de Madrid, Av. Universidad, 30, Leganés, Spain, blanco.sanchez.joaquin@gmail.com

David Álvarez Sánchez
Universidad Carlos III de Madrid, Av. Universidad, 30, Leganés, Spain, dasanche@ing.uc3m.es

Fernando Martín Monar
Universidad Carlos III de Madrid, Av. Universidad, 30, Leganés, Spain, fmmonar@ing.uc3m.es

Luis E. Moreno Lorente
Universidad Carlos III de Madrid, Av. Universidad, 30, Leganés, Spain, moreno@ing.uc3m.es

Abstract

This paper presents the calibration and integration of Inasutoma sensors, a specific model of Force Sensing Resistors (FSRs), in the robotic hand Gifu Hand III. After an initial sensor behavior observation, a calibration strategy was designed and a mathematical model defining it was described. Once the behavior was known, the sensors were integrated in the robotic hand. For this purpose new fingertips were designed and the sensors were integrated in their surface. They were later covered with a Polydimethylsiloxane rubber to improve grasping properties. This whole structure was assembled in the robotic hand Gifu Hand III.

Key words: Force Sensing Resistors (FSRs), robotic hand, Polydimethylsiloxane (PDMS).

1 INTRODUCTION

Different anthropomorphic robot hands with completely mechanical functionality have been developed during the last decade. This mechanical functionality tries to mimic human grasping and manipulation capabilities, which are achieved thanks to what is known as *set of three oppositions*: pad, for forces between the pads of the fingers and the thumb; palm, for forces between fingers and the palm; and side, for forces between the thumb and the side of the index finger [8]. These oppositions are used either separately or simultaneously to carry out different tasks where the geometry of the handgrip and the power applied change depending on the specific task. However, a good mechanical design is not enough for most types of interaction with the environment. Both haptic and kinematic sensing are very important in order to be able to perform more accurate actions regarding either grasping and manipulation.

In robotics, touch sensing is defined at a single contact point. Cutaneous and kinesthetic systems in the human body are called, in robotics, the extrinsic and intrinsic touch systems respectively. Both are achieved through tactile sensors, but extrinsic sensors are located at the contact surface while intrinsic sensors are located within the mechanical structure. The term tactile sensing is usually used to refer to external touch sensing in robotics. Crago et al. [10] stated that the principal ideal requirements of an artificial force sensor usable for the characterization of the grasp forces are: 1) operating range between 0.1 and 80 N; 2) resolution of 0.1 N for light load and 1 N in case of heavy load; 3) repeatability; and 4) stability.

Several types of transduction methods have been used to achieve tactile sensing for robotic applications. In [4], a resistive sensor is used to cover a whole robotic system acting as a skin, but they need high power consumption and do not provide local contact measurement. Quantum Tunnel Composites (QTCs) are being used in tactile arrays for dynamic pressure distribution measurement [13], however, they have a highly non-linear response. Capacitive sensors are very used in the technological market for human interface devices and are also used in robotics as embedded artificial skin for humanoid robots [2], although they need complex electronics to be used and present hysteresis in the measurement. Optical sensors, recently used by [3] as human touch, require complex computations although they present flexibility, which is good for adapting to different shapes. Force Sensing Resistors (FSRs), a piezoresistive type of sensor, are used in many tactile systems for measuring external forces [12,1,5]. They

ISBN 978-84-15914-12-9

present good characteristics such as robustness, flexibility and low cost.

Gifu Hand III was designed by Kawasaki and Mouri Laboratoy, at Gifu University. It is a light anthropomorphic hand with 5 fingers driven by built-in actuators [10]. All joints include angular position sensing, but no tactile sensing is included in the hand.

This work describes the integration of FSR type sensors force sensors in the fingertips of Gifu Hand III. Previously, the sensors' response has been mathematically modeled. Besides the structure of the fingertips has been modified in order to achieve a more anthropomorphic design. Last, the sensors have been covered with Polydimethylsiloxane (PDMS), a plastic rubber that improves the grasping capability of the fingertips thanks to its compliance and friction to contact.

The next sections of the paper are organized as follows. Section 2 describes the calibration and mathematical modeling for the sensors. The integration of the sensors in the newly design fingertips and the cover with the rubber is explained in section 3. Finally, in section 4 conclusions and future work are addressed.

2 CALIBRATION

2.1 CALIBRATION SYSTEM

The sensor to be calibrated, the *Inasutoma* sensor, has a sensing area of 8 mm covered by a rubber dome that helps to evenly distribute the force applied over its entire surface, allowing to measure pressure and avoiding the sensor to become saturated from punctual applied loads [6].

2.1.1 Data gathering system

The sensor was connected to a voltage divider circuit for high resolution and low value range measurements. This is achieved by chosen a 1kΩ resistor as measuring resistor, maximizing the sensitivity in the work range and limiting the current through the sensor [7].

A specific calibration system was designed with Tinkercad software and later 3D printed. Its specific assembly can be seen in Figure 1.

By placing weights on the flat surface, a compression force is generated and completely transmitted through the frustum, which has a small surface of 8mm just as the sensing area of the sensor. The final implementations includes a scale in order to ensure that the weight is being placed correctly on the flat surface and therefore that there is no force lost due to geometry (Figure 1, right).

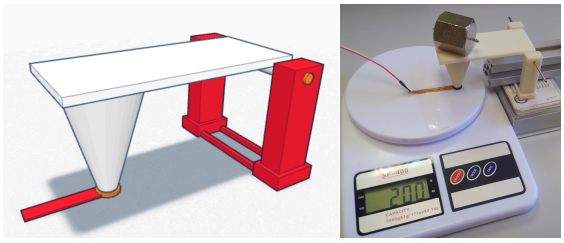

Figure 1: 3D sketch of the calibration system (left) and real calibration system implementation (right)

A STM32F4 microprocessor was programmed for data acquisition and processing. The program both plots the signal in real time and stores it for post-processing with a sampling rate of 100 samples per second.

2.1.2 Methodology

Ten measurements were taken in the 0–1000 grams range, which was covered with 200g weights up to 1000g. They were placed on top of each other one by one and later removed one by one too to see the hysteresis behavior of the sensor. Five measurements were taken in the 0 – 200 grams range, which was covered with 40g weights up to 200g. This smaller range was covered because the sensitivity of the sensor is bigger at low weights than at high weights.

Calibrated weights were placed over the flat surface to obtain a relation between the applied force and the output voltage of the circuit. The handling of the weights was manual and very delicate and as consequence some noise was introduced in the measurement. This noise was removed during post-processing of the data. A first step of this processing includes a mean filter that is run through the stored data. Due to the sampling rate, ten measurements are obtained for each 0.1 seconds. The mean filter provides with the mean of these ten values so that only one value for each 0.1 second is considered.

2.2 RESULTS AND INTERPRETATION

For clarification purposes graph of Trial 3 in the range 0–1000g, shown in Figure 2, will be explained in detail. For every graph there are two different parts that have been called Part 1 and Part 2. Part 1 corresponds to measurements performed in the 0–1000g range by increasing the weight applied from 0 to 1000 g, while Part 2 corresponds to measurements also performed in the same range but in this case by decreasing the weight from 1000 to 0 g. Part 1 will be used to define the mathematical model describing the response of the sensor for any weight. Part 2 will

ISBN 978-84-15914-12-9

be used to see and understand the Hysteresis behavior of the sensor.

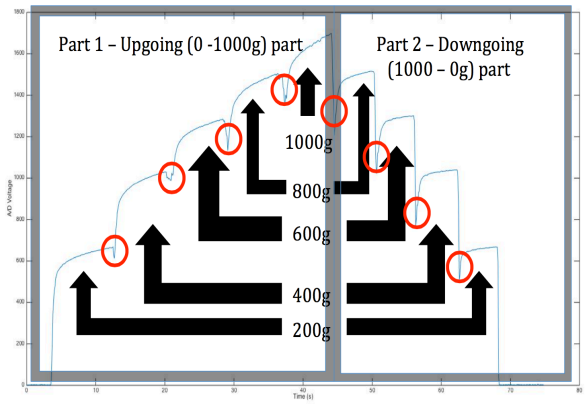

Figure 2: Trial 3 explanatory graph

With these results, two conclusions are obtained. First, the sensor does not reach a saturation value but a saturation rate; this means that a final constant value is not reached; instead a final growth rate is. However, the values obtained from the point where this rate is reached can be neglected since manipulation and grasping of objects with a robotic hand is a short-length task. The proposed mathematical models, in section 2.3, do not hold true for infinite time but it does for short time applications. Second, the peaks appearing between two consecutive weights, marked with red circles in Figure 2, are not due to the behavior of the sensor but to the manual handling of the weights during the calibration. They must not be taken into account.

The calibration method designed showed that the *Inasutoma* sensor has a step response that changes for each weight applied comparable to that of a first order system. They are characterized by two different parameters: the gain $\boldsymbol{k}$ and the time constant $\boldsymbol{\tau}$. The gain is determined by the magnitude of the output when a known input is applied, while the time constant is determined by how fast the system reaches the magnitude of the output. The response of the sensor follows the formula in Equation 1:

$$\text{A/D Voltage} = \text{k} * (1 - \text{e}\text{\^{}}(-\text{t}/\tau)) \qquad (1)$$

In order to find k and τ, every trial had to be divided in five parts according to each weight (200, 400, 600, 800 and 1000g). By plotting all parts for the same trial in one plot as shown in Figure 3, a pattern for k and τ can be inferred: as the weight/force applied is increased, k must decrease and τ must increase. Further analysis, which can be found in next section 2.3, confirmed this hunch.

The same study was performed with Part 2 of each graph. The values obtained for this part of the graph are slightly different. It was known beforehand that these sensors presented Hysteresis behavior and it was confirmed with this study. This procedure was as well repeated for the measurements in the 0–200g range and the same pattern for $\boldsymbol{k}$ and $\boldsymbol{\tau}$ was observed.

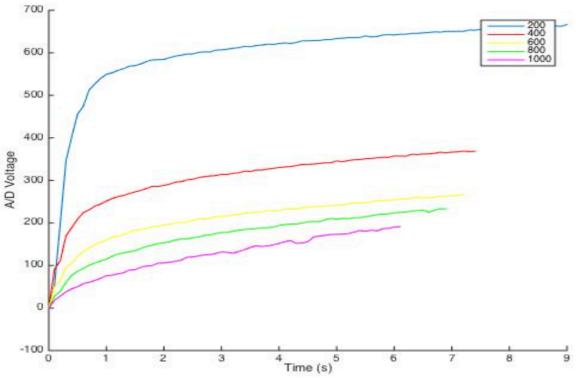

Figure 3:Trial 3 – Separated parts for 200, 400, 600, 800 and 1000g corresponding to Part 1

2.3 MATHEMATICAL MODELS

Several steps are required for the adjustment of a mathematical model. The first one is to manually find the values of $\boldsymbol{k}$ and $\boldsymbol{\tau}$ for each weight and each trial that model a first order system as close as possible to the real measured response. Both of them were calculated and later introduced in a MATLAB script for modeling of the first order systems that will be used for comparison with the real values obtained. The second step is to statistically adjust these values to find those that reduce the Mean Square Error.

Variable $\boldsymbol{k}$ can be calculated straight forward from the measurements with formula in Equation 2:

$$\text{k} = \frac{\text{V}_{\text{final}} - \text{V}_{\text{initial}}}{\text{Weight}} \qquad (2)$$

where V_{final} is the A/D voltage value in the last measurement, $V_{initial}$ is the voltage in the first measurement, and Weight is the actual weight sensed by the scale (previously wrote down during the recording of the measurements).

Calculating $\boldsymbol{\tau}$ is a rougher process than calculating $\boldsymbol{k}$. Originally $\boldsymbol{\tau}$ corresponds to a 63.7% of the time it takes the system to reach the final value. It is known that the *Inasutoma* sensor does not behave as a first order system for long times and therefore the final value recorded does not correspond to the interesting behavior of the sensor. Accordingly the value of $\boldsymbol{\tau}$ had to be adjusted to obtain a curve as close as possible to that seen in the real measurement. This was achieved by multiplying $\boldsymbol{\tau}$ by a variable

ISBN 978-84-15914-12-9

parameter *c* smaller than 1. This parameter actually reduces the total measured time so it matches the point where the sensor stops behaving as a first order system. The final formula to calculate $\boldsymbol{\tau}$ is presented in Equation 3:

$$\tau = c \cdot (0.637 \cdot t_{total}) \qquad (3)$$

where t_{total} is the time elapsed from the first measurement to the last one taken into account. Figure 4 shows an example of comparison between the real response of the sensor and the modeled response of the sensor. It corresponds to Trial 9 of 0–1000g range with a 1000g weight.

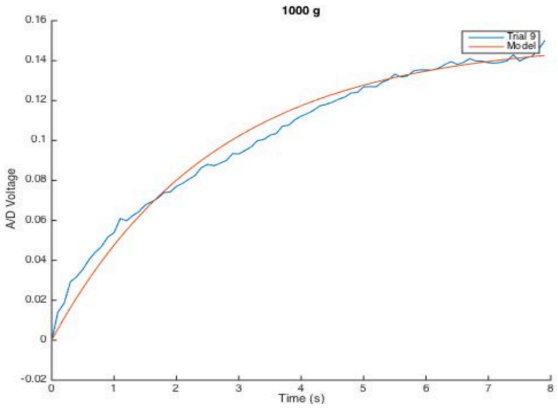

Figure 4: Trial 9 – Modeled response vs. Real response

Furthermore once the values of $\boldsymbol{k}$ and $\boldsymbol{\tau}$ had been obtained for each trial and weight, the mean values for each weight were calculated. With these values a modeled response for each weight was calculated. The next logical step was to calculate the error presenting these models and to try to minimize it. For this purpose the Mean Square Error (MSE) is calculated and a search is performed to find the combination of $\boldsymbol{k}$ and $\boldsymbol{\tau}$ values that minimizes the error for each generated model.

The MSE is an indicator of the difference between the estimator (the real response of the sensor) and what is estimated (modeled response of the sensor). The Formula in Equation 4 is used to calculate the MSE for each weight:

$$MSE = \sqrt{\frac{1}{N}\sum_{i=1}^{j}\sum_{m=1}^{W}|V_{trial\,n}(i) - V_{model}(i)|^2} \qquad (4)$$

where *j* is the minimum length of the measurement vectors to ensure that the same number of samples is taken from each trial. *N* is the total number of samples taken into account and can be easily obtained by simply multiplying *j* by the number of trials (ten for the 0–1000g range and five for the 0–200g range), and *W* is the number of trials. For example, the model shown in Figure 3 has a *MSE = 0.0852*.

Now it must be analyzed if there happens to be a different combination of $\boldsymbol{k}$ and $\boldsymbol{\tau}$ that reduces the MSE for each model. A search that goes over all possible combinations of $\boldsymbol{k}$ and $\boldsymbol{\tau}$ is performed. The area chosen is the one enclosed by the rectangle formed between the minimum and maximum values of these parameters. The obtained values of $\boldsymbol{k}$ and $\boldsymbol{\tau}$ minimizing the error will be used to generate a new model for each weight. Figure 5 shows the model minimizing the error for the 1000g weight.

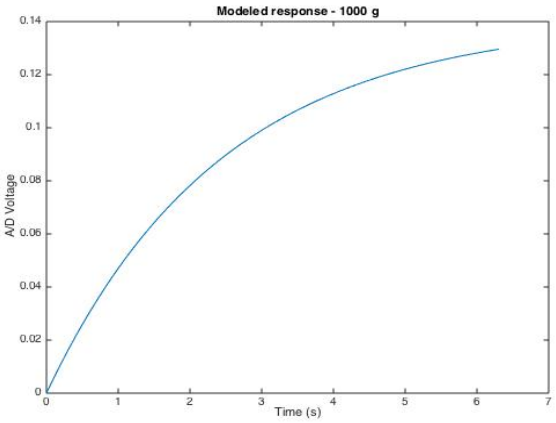

Figure 5: Modeled response for 1000g with values of $\boldsymbol{k}$ and $\boldsymbol{\tau}$ minimizing the error

Once the most accurate values of $\boldsymbol{k}$ and $\boldsymbol{\tau}$ were obtained, the fashion of their behavior could be seen and adjusted in a curve. Figure 5 shows the fashion curve followed by $\boldsymbol{\tau}$ in the interval 0–1000g. The mathematical equations describing their fashions could be used to obtain $\boldsymbol{k}$ and $\boldsymbol{\tau}$ for any desired value and therefore to obtain a modeled response of the sensor for any weight. The obtained values for $\boldsymbol{k}$ and $\boldsymbol{\tau}$ minimizing the error for each weight in both ranges, 0–1000g and 0–200g, and their respective MSE are shown in Table 1 and Table 2.

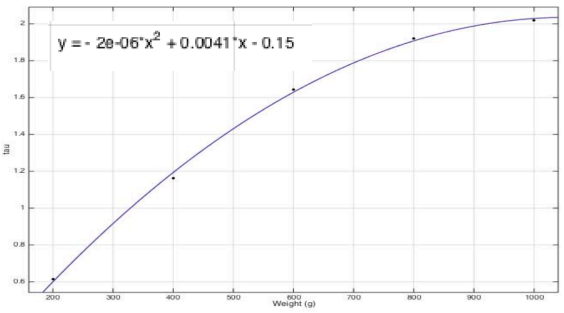

Figure 6:Fashion followed by $\boldsymbol{\tau}$ in the interval 0–1000g and the mathematical equation describing it

ISBN 978-84-15914-12-9

Table 1: k, τ, and MSE values in the 0–1000g range

Weight (g)	k	τ	MSE
200	3.042	0.6128	0.2483
400	0.640	1.1625	0.1727
600	0.302	1.1642	0.1381
800	0.222	1.9206	0.1818
1000	0.150	2.0206	0.0836

Table 2: k, τ, and MSE values in the 0–200g range

Weight (g)	k	τ	MSE
40	6.6085	0.49	0.5632
80	1.6013	0.93	0.2413
120	0.6875	1.61	0.0794
160	0.5191	1.70	0.05961
200	0.4190	0.86	0.08115

3 INTEGRATION OF INASUTOMA SENSORS IN GIFU HAND III

Contrary to what you might expect, integration of the sensors in the robotic hand is not a straightforward process that must ensure the best performance of the formers.

3.1 FINGERTIPS

New fingertips were designed in order to mimic anthropomorphic shape of human hand and in order to facilitate the attachment of the sensors.

The original fingertips of Gifu Hand III are completely round, which makes them anatomically inconsistent and unpractical for sensor attachment since they do not present any planar surface. Moreover their surface is sliding, which makes grasping of objects a complicate process.

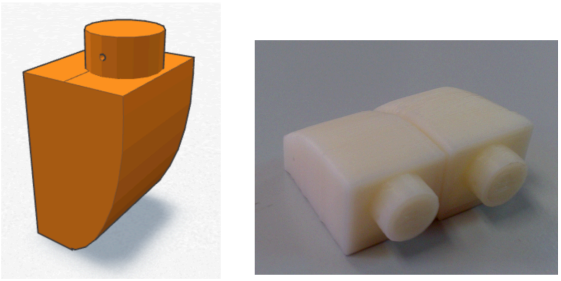

Figure 7: Fingertip 3D sketch (left) and real 3D printed fingertips (right)

With this information, it was decided to design and again 3D print new fingertips. Two main parameters were considered for the design. The first one is the plastic used for 3D printing and the second one is the curvature of the finger. The former is Poly-Lactic-Acid (PLA), which produces rough surfaces. The later was measured and compared among different individuals and adjusted to the size of the Gifu Hand III. The designed 3D sketch of the new fingertip (left), as well as the final piece (right) are shown in Figure 7.

The most remarkable characteristics are its non-sliding surface that not only eases sensor attachment but also improves grasping of objects, and its anatomical consistency that allows for more real object-hand interactions.

3.2 POLYDIMETHTYLSILOXANE (PDMS)

The surface of the fingertips where the sensors will be attached will be covered with a rubber to improve performance. Rubbers increase compliance, how well the sensor adapts to the shape of the object, as well as the grip ability of the surface.

The chosen rubber was Polydimethylsiloxane (PDMS) since its properties and way of fabrication could be easily adapted. Late studies are starting to show tactile sensors that use PDMS as the dome to improve performance [8].

PDMS is a polymeric compound that belongs to the group of silicones. It presents some interesting properties that justify its use in this application. First, PDMS is inexpensive. Second, PDMS can be shaped during fabrication process and therefore it can be adapted to most surface and shapes, like in this case the surface of the fingertips with the sensors attached. Third, PDMS roughness is similar to the skin, producing a more natural object-surface interaction. Fourth, PDMS elasticity can be controlled with the polymer-curing agent mixing ratio. Fifth, PDMS is soft and therefore unlikely to damage other surfaces, eliminating the risk of damaging the sensors. Sixth, PDMS is biocompatible ensuring user safety.

During the fabrication process of the covers for the fingertips three main materials were used: Sylgard polymer, curing agent and puffy paint. PDMS is formerly obtained by mixing and curing Sylgard polymer with the curing agent while puffy paint is used to create 3D shapes in the PDMS.

First, the sensor shape was drawn in a petri dish with puffy paint that hardens after heating. The petri dish was placed in the oven for this purpose. Second, PDMS gel was produced by mixing Sylgard polymer with curing agent. As stated before their mixing ratio determines the elasticity of the final PDMS product. Thorough mixing of the two components is essential

ISBN 978-84-15914-12-9

for good curing. Third, the PDMS gel was poured in the petri dish with the puffy paint pattern. Some bubbles appear and they might be removed by using a vacuum chamber. Note that bubbles only affect to optical properties of PDMS, which are not of interest here. Fourth, the petri dish was placed in the oven for curing. Once cured the PDMS becomes an elastic solid that thanks to the puffy paint pattern has 3D cavities. This allows the cover to perfectly adapt to the sensors attached to the fingertips.

Two different PDMS covers were created. One designed to include one sensor per fingertip and another one designed to include two sensors per fingertip. This last one is shown in Figure 8. The only difference during the fabrication process is the pattern drawn in the petri dish with the puffy paint. Both structures were designed to give 3D shapes to the PDMS in such a way that the cavities introduced are later filled with the dome of the sensors.

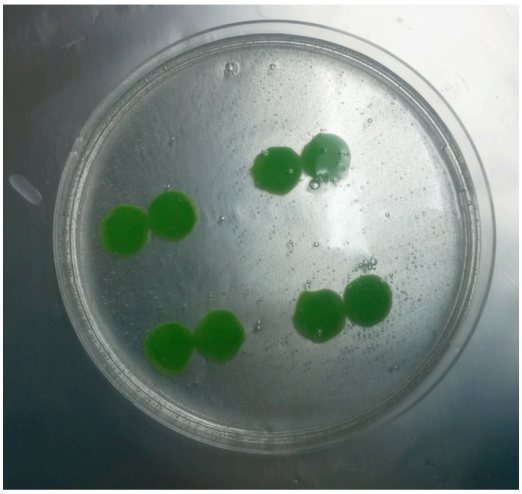

Figure 8: PDMS on petri dish with pattern for two sensors drawn with Green puffy paint

3.3 ASSEMBLY

The last step in the integration is the assembly of the three different parts (the sensors, the fingertips and the PDMS covers) together, and then the assembly of this structure in the Gifu Hand III.

The sensors were attached to the surface of the fingertips by gluing their flexible board since their integrity is not compromised and it is a reversible process.

The PDMS in the petri dish must be unmolded and cleaned in order to wash off any remainder of the puffy paint. This can be easily performed by rinsing the surface with water since PDMS is chemically resistant. Then the petri dish was cut into pieces whose dimensions match those of the fingertip surface and also that the cavities introduced match the position of the sensors. The PDMS cover was glued to the surface in the points where it is not in contact with the sensor.

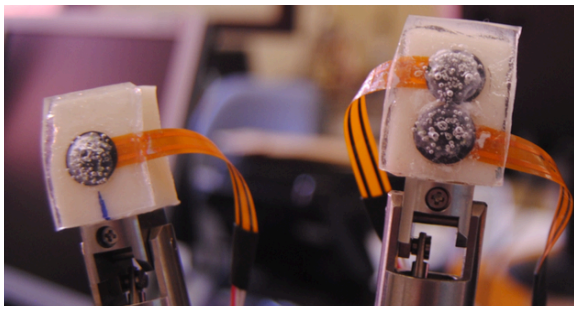

Figure 9:Sensors integrated in the robotic hand Gifu Hand III

This structure was screwed to the hand with the holes previously introduced in the 3D-printed fingertip, although they had to be widened in order to reuse the original screws. The final assembly is shown in Figure 9 and Figure 10. Figure 10 shows that there is no hump between the PDMS cover and the sensor as expected due to the 3D cavities introduced in the PDMS cover.

Figure 10: Lateral view of final assembled structure showing no hump in the surface of the PDMS

4 CONCLUSIONS AND FUTURE WORK

This paper is focused in the proper calibration and integration of the *Inasutoma* sensors in the robotic hand Gifu Hand III.

A calibration method was designed for mathematical modeling of the behavior of the sensors. This method implies a 3D printed calibration system adjusted to the dimensions of the sensor.

The data gathered from the two different calibration ranges showed that the sensor acts as a first order system whose behavior could be mathematically described. The models still present some error that is

ISBN 978-84-15914-12-9

analyzed with the Mean Square Error. This error is in big part introduced by the hysteresis behavior of the sensor.

After the calibration of the sensors, they were integrated in the hand. New fingertips were designed and 3D printed to replace the original ones. Although these fingertips are anatomically consistent in the region of interest, some improvement could be performed in the general design for aesthetic reasons. The sensors were attached to the fingertips and later covered with PDMS to improve grasping properties. This later process could be improved by curing PDMS in molds perfectly adapted to the shape of the fingertips.

Future work lines will follow different steps. First, the calibration process must be automatized in order not to introduce noise derived from manual handling of the weights. Second, new PDMS covers will be designed and tried on the hand. This includes changing the mixing ratio to control PDMS elasticity and also changing the amount of PDMS poured into the petri dish to control the thickness. Third, the behavior of the sensors with the PDMS covers will be analyzed to check whether the described mathematical models still hold true or if some adjustment is needed. And third, trials of hand grasping and manipulation of objects will be performed. This will check if repositioning of the sensors within the fingertip surface is needed or if the surface needed to be redesign for proper contact.

Acknowledgments

This work is funded by the project number DPI2010-17772, by the Spanish Ministry of Science and Innovation, and also by RoboCity2030-III-CM project (Robtica aplicada a la mejora de la calidad de vida de los ciudadanos. fase III; S2013/MIT-2748), funded by Programas de Actividades I+D en la Comunidad de Madrid and co-funded by Structural Funds of the EU.

References

[1] D.J. Beebe, D.D. Denton, R.G. Radwin and J.G. Webster, “A silicon-based tactile sensor for finger-mounted applications”, IEEE Trans Biomed Eng, vol. 45, no. 2, pp. 151-159, 1998.

[2] Giorgio Cannata, Marco Maggiali, Giorgio Metta, Giulio Sandini. "An Embedded Artificial Skin for Humanoid Robots." *International Conference on Multisensor Fusion and Integration for Intelligent Systems.* Seoul, Korea: IEEE, 2008. 434-438.

[3] Hanafiah Yussof, Jiro Wada, Masahiro Ohka. "Analysis Of Tactile Slippage Control Algorithm For Robotic Hand Performing Grasp-Move-Twist Motions." *International Journal on Smart Sensing and Intelligent Systems* 3, no. 3 (September 2010): 359-375.

[4] Heinz Wörn, Karsten Weiß. "The Working Principle of Resisitive Tactile Sensor Cells." *International Conference on Mechatronics & Automation.* Niagara Falls: IEEE, 2005. 471-476.

[5] I. Gaiser, S. Schulz, A. Kargov, H. Klosek, A. Bierbaum, C. Pylatiuk, R. Oberle, T. Werner, T. Asfour, G. Bretthauer, R. Dillmann. "A New Anthropomorphic Robot Hand." *International Conference on Humanoid Robots.* Deajeon, Korea: IEEE, 2008. 418-422.

[6] INABA RUBBER Co. Ltd. *INASTOMER (Pressure Conductive Sensor)*. Retrieved July 14, 2015 from Detection of rolling and writing pressure Contact, Gap and Narrow part detection: http://www.inaba-rubber.co.jp/en/b_products/inastomer/sf.html

[7] Interlink Electronics. "FSR Force Sensing Resistors." *FSR Integration Guide.* Camarillo, CA.

[8] King Fong Lei, Kun-Fei Lee, Ming-Yih Lee. "A flexible PDMS capacitive tactile sensor with adjustable measurement range for plantar pressure measurement." Microsystem Technologies (Springer), no. 20 (September 2013): 1351-1358.

[9] M.R. Cutkosky, R.D. Howe. *Human Grasp Choice and Robotics Grasp Analysis.* Vol. 1. Springer-Verlag, 1990.

[10] P.E. Crago, H.J. Chizeck, M.R. Neuman and F.T. Hambrecht, “Sensors for use with functional neuromuscular stimulation”, IEEE Trans Biomed Eng, vol. 33, pp. 256-268, 1986.

[11] Robot hand - unit for research. *Robot hand – unit for research.* http://robothand.eu/en/products/robotic_hands/robot_hand_gifu_hand_iii/ (accessed April 20, 2105).

[12] T.R. Jensen, R.G. Radwin and J.G. Webster, “A conductive polymer sensor for measuring external finger forces”, J Biomechanics, vol. 24, no. 9, pp. 851-858. 1991.

ISBN 978-84-15914-12-9

[13] YWR Amarasinghe, AL Kulasekera, TGP Priyadarshana. "Quantum Tunneling Composite (QTC) Based Tactile Sensor Array For Dynamic Pressure Distribution Measurement." *Seventh International Conference on Sensing Technology (ICST)*. Wellington: IEEE, 2013. 1-4.